Inhibition of NADH Oxidation by 1-Methyl-4-phenylpyridinium Analogs as the Basis for the Prediction of the Inhibitory Potency of Novel Compounds

Sergey O. Sablin,[1,2] Matthew J. Krueger,[1,2] Victoria L. Yankovskaya,[1,2] Sergey E. Tkachenko,[4] Alexander N. Razdolsky,[4] Sergey O. Bachurin,[4] Rona R. Ramsay,[1,2,] and Thomas P. Singer[1,2,3]*

[1]Molecular Biology Division, Veterans Affairs Medical Center, San Francisco, CA 94121; [2]Department of Biochemistry and Biophysics, and [3]Division of Toxicology, University of California, San Francisco, CA 94143; and [4]Institute for Physiologically Active Substances, Russian Academy of Sciences, Chernogolovka, Moscow Region, 142432, Russia

ABSTRACT: Inhibition of NADH dehydrogenase (Complex I) of the mitochondrial respiratory chain by 1-methyl-4-phenylpyridinium (MPP^+) and its analogs results in dopaminergic cell death. In the present study, the inhibition of mitochondrial respiration and of NADH oxidation in inverted inner membrane preparations by the oxidation products of *N*-methyl-stilbazoles (*N*-methyl-styrylpyridiniums) are characterized. These nonflexible MPP^+ analogs were found to be considerably more potent inhibitors than the corresponding MPP^+ derivatives. The IC_{50} values for these compounds and previously published figures for MPP^+ analogs were then used to select a computer model based on structural parameters to predict the inhibitory potency of other compounds that react at the "rotenone site" in Complex I. A series of 12 novel inhibitors different in structure from the basic set were used to test the predictive capacity of the models selected. Despite major structural differences between the novel test compounds and the MPP^+ and styrylpyridinium analogs on which the models were based, substantial agreement was found between the predicted and experimentally determined IC_{50} values. The value of this technique lies in the potential for the prediction of the inhibitory potency of other drugs and toxins which block mitochondrial respiration by interacting at the rotenone sites. © 1996 John Wiley & Sons, Inc.

KEY WORDS: **Complex I Inhibitor, Rotenone Sites, Structure-Activity Relations, Styrylpyridinium Inhibitors.**

INTRODUCTION

Expression of the neurotoxicity of *N*-methyl-4-phenyl-tetrahydropyridine (MPTP) and of its analogs is initiated by a four-electron oxidation to the pyridinium forms, catalyzed by monoamine oxidase A or B, or both, depending on the structure of the MPTP derivative (1). The resulting pyridinium, *N*-methyl-4-phenylpyridinium (MPP^+) in the case of MPTP, is then taken up by the presynaptic dopamine carrier and concentrated by the electrochemical gradient of the inner membrane into the mitochondrial matrix (2). There it combines with NADH dehydrogenase (NADH-ubiquinone reductase) in the same domain as rotenone and piericidin A (3, 4) and blocks electron transport from the high potential iron–sulfur cluster of the enzyme to ubiquinone (5, 6).

Several laboratories have studied the relation of neurotoxicity to the structure of MPP^+ analogs or of the parent tetrahydropyridines in attempts to define the minimal requirements for neurotoxicity. It has been found that alterations in the pyridine ring of MPTP or lengthening the alkyl substituent on the nitrogen generally lessens or abolishes the neurotoxicity, probably because such analogs are not oxidized significantly by MAO A or B, but certain substitutions in the aromatic ring do not result in loss of the inhibitory potential (7–9). In the present article, we report that rigid MPP^+ analogs (*N*-methyl-4-styrylpyridiniums) are effective inhibitors of mitochondrial respiration on NAD^+-

Received February 9, 1996.

Address correspondence and reprint requests to Thomas P. Singer, Department of Veterans Affairs Medical Center, 4150 Clement Street, 151-S, San Francisco, CA 94121. Tel.: (415) 752-9676; Fax: (415) 750-6959.

*Current address: School of Biological and Medical Sciences, University of St. Andrews, Irving Building, North St., St. Andrews, FIFE KY16 9AL, Scotland.

0887-2082/96/010033-11

linked substrates and that most of them also inhibit NADH oxidation in inverted membranes with a lower IC_{50} value than MPP^+ itself. In the light of these and previously reported data, there is a sufficient variety of structures to select a model based on common physical parameters to use for the prediction of the inhibitory potency of structurally related but untested compounds.

MATERIALS AND METHODS

The inhibitors were synthesized in the Institute of Physiologically Active Substances, Russian Academy of Science, Chemogolovka, Russia. *N*-ethyl-4-phenylstyrylpyridinium and *N*-benzyl-4-phenylstyryl-pyridinium were synthesized as previously described for the *N*-methyl compound (10), except that ethyl iodide and benzyl chloride were used instead of methyl iodide. All other compounds were synthesized, and the purity was controlled as already described (10–12).

The novel inhibitors shown in Figure 4 and used in the experiments reported in Table 2 were prepared as follows: Compounds **1** and **2** were synthesized, in 40 and 85% yield, respectively, from piperidine by reaction with the appropriate alkyl or benzyl halogenide. Compound **3** was synthesized, in 40% yield, from the dichloroanhydride of adipic acid by reaction with dimethylaminoethanol, followed by quaternization with methyl iodide. Compounds **4** and **5** were synthesized in 60 and 19% yield, respectively, from 1-naphthol, trimethylamine and either 1,2-dibromoethane (**4**) or epichlorohydrine (**5**) by a similar protocol, except that for compound **4**, the 2-bromoethyl-1-naphthyl ether was synthesized, and the triethylamine was added, whereas for compound **5**, epichlorohydrine was added dropwise to a mixture of 1-naphthol and trimethylamine. Compound **12** was synthesized in 23% yield from 1-naphthol, triethylamine, and epicholohydrine, followed by reaction with benzyl chloride. Compounds **6–11** were synthesized, in 50–95% yield, by methylation of the appropriate ester or anilide of isonicotinic acid. All the compounds were characterized by ^1H NMR, elementary analysis, and melting point. These compounds are potentially neurotoxic so that aerosols and skin contact must be avoided. Analytical data are summarized in the following:

1. *N*-Benzyl-*N*-butylpiperidinium chloride (**8**): yield 40%; mp 177–178°C; ^1H NMR (D_20, extn TMS): 0.94 (t, 3H, CH_3); 1.33 (m, 4H); 1.54–1.7 (m, 3H); 1.84 (m, 4H); 3.33 (m, 6H); 4.58 (s, 2H); 7.50 (m, 5H, H_{arom}).
2. *N*-Methoxyethyl-*N*-propylpiperidinium iodide: yield 85%; mp 146–147°C; ^1H NMR (D_20, extn TMS): 0.93 (t, 3H, CH_3); 1.57–1.75 (m, 4H); 1.85 (m, 4H); 3.35 (m, 6H); 3.40 (s, 3H, OCH_3); 3.54 (m, 2H, AA'BB', NCH_2–CH_2); 3.83 (m, 2H, AA'BB', CH_2–CH_2O).
3. Choline diester of adipec acid diodide: yield 85%; mp 138–140°C; (D_2O, extn TMS): 0.74 (t, 4H, CH_2CO); 2.46 (t, 4H, CH_2CH_2O); 3.21 (s, 9H, CH_3); 3.67 (t, 4H, CH_2N); 4.56 (t, 4H, CH_2O).
4. *N*-2-(1-Naphthoxy)ethyl-*N,N,N*-trimethylammonium bromide: yield 33%; mp 182–186°C; ^1H NMR (D_2O, extn TMS): 3.0 (s, 9H); 3.5 (m, 2H); 4.18 (m, 2H); 6.64 (m, 1H); 7.16–7.44 (m, 4H); 7.6 (m, 1H); 7.9 (m, 1H).
5. *N*-2-[(1-Naphthoxy)-2-hydroxypropyl]-*N,N,N*-trimethylammonium bromide: yield 19%; mp 217–220°C; ^1H NMR (D_2O extn TMS): 3.1 (s, 9H); 3.5 (m, 2H); 4.0 (m, 2H); 4.45 (m, 1H); 6.67 (m, 1H); 7.14–7.54 (m, 4H); 7.72 (m, 1H); 8.1 (m, 1H).
6. Methyl isonicotinate methiodide: yield 95%; mp 173–175°C; ^1H NMR (D; i2O, extn TMS): 2.9 (s, 3H, CH_3), 4.46 (m, 3H, N–CH_3), 8.51 (d, 2H, J = 7 Hz, β-H-pyridyl), 8.95 (d, 2H, J = 7 Hz, α-H-pyridyl).
7. Ethyl isonicotinate methiodide: yield 95%; mp 127–129°C; ^1H NMR (D_2O extn TMS): 1.36 (t, 3H, CH_3), 4.44 (m, 5H, CH_2 + N–CH_3), 8.50 (d, 2H, J = 7 Hz, β-H-pyridyl), 8.98 (d, 2H, J = 7 Hz, α-H-pyridyl).
8. Iso-propyl isonicotinate methiodide: yield 85%; mp 120–121°C; s1H NMR (D_2O, extn TMS): 1.34 (d, 6H, $2CH_3$), 4.40 (s, 3H, N–CH_3), 5.22 (m, 1H, CH), 8.44 (d, 2H, J = 7 Hz, β-H-pyridyl), 8.90 (d, 2H, J = 7 Hz, α-H-pyridyl).
9. Anilide *N*-methyl-isonicotinate iodide: yield 75%; mp 148–150°C; ^1H NMR (D_2O, extn TMS): 4.43 (s, 3H, CH_3); 7.63 (m, 5H, phenyl), 8.33 (d, 2H, J = 7 Hz, β-H-pyridyl), 8.91 (d, 2H, J = 7 Hz, α-H-pyridyl).
10. Phenyl isonicotinate methiodide: yield 85%; mp 210°C; ^1H NMR (Me_2SO-d6); 4.53 (s, 3H, CH_3), 7.31–7.61 (m, 5H, phenyl), 8.72 (d, 2H, J = 8 Hz, β-H-pyridyl), 9.28 (d, 2H, J = 8 Hz, α-H-pyridyl).
11. 2-Naphthyl isonicotinate methiodide: yield 50%; mp 230–232°C; ^1H NMR (Me_2SO-d6); 4.58 (s, 3H, CH_3), 7.63–7.80 (m, 3H, 2,3,10-H-naphthyl), 8.02–8.28 (m, 4H, 5,6,7,8-H-naphthyl), 8.86 (d, 2H, J = 7 Hz, β-H-pyridyl), 9.38 (d, 2H, J = 7 Hz, α-H-pyridyl).
12. *N*-3-(1-Naphthoxy)-2-benzoxypropyl-*N,N,N*-triethylammonium chloride: yield 23%; ^1H NMR (D_2O, extn TMS): 0.93 (t, 9H, CH_3), 2.93 (m, 8H, N–CH_2), 3.95 (m, 3H, CH–CH_2O), 4.21 (s, 2H, CH_2–Ph), 6.60 (m, 1H, naphthyl), 6.94 (br s, 5H, phenyl), 7.0–7.3 (m, 5H, naphthyl), 8.0 (m, 1H, naphthyl).

Rat liver mitochondria were prepared by the method of Schnaitman and Greenawalt and inner

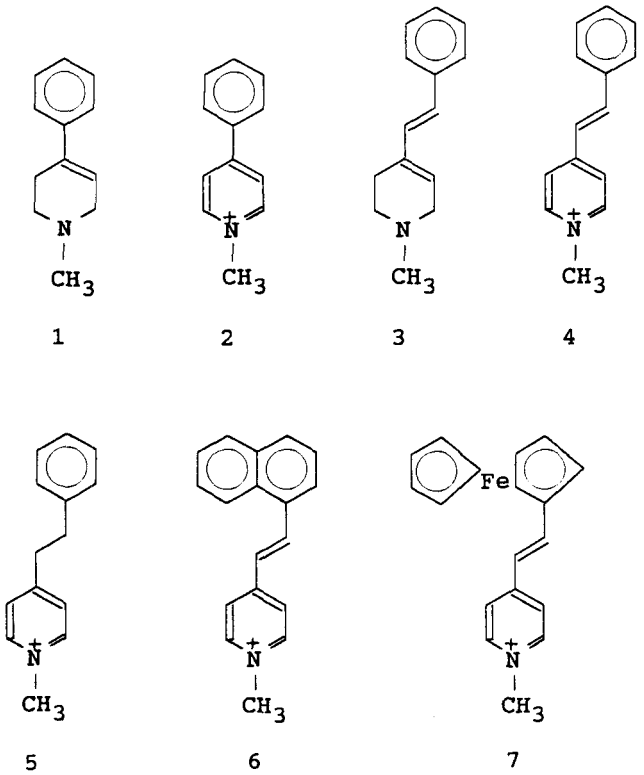

FIGURE 1. Structures of the compounds shown in Table 1 as such or in substituted forms. **1** = MPTP; **2** = MPP^+; **3** = MTHS; **4** = MSP^+; **5** = 1-Me-4-(phenylethyl)-P^+; **6** = 1-Me-4-(α-naphthylethyl)P^+; **7** = 1-Me-4-(α-ferrocenylethenyl)P^+.

membranes from beef heart mitochondria (ETP) as described (13, 14). Mitochondrial respiration on malate plus glutamate was measured polarographically at 30°C, as in previous work (2), after a 5 minute preincubation with or without inhibitor. The oxidation of NADH (0.28 mM) by ETP was also assayed polarographically at 30°C in the presence of 0.2 mg membrane protein/mL (15).

RESULTS

Inhibition of State 3 Respiration in Mitochondria

The 1-methylstyrylpyridiniums are nonflexible analogs of MPP^+, as shown in Figure 1. When mitochondria oxidizing NADH-linked substrates are preincubated with MSP^+, inhibition develops slowly (Figure 2), as was observed for MPP^+. The degree of inhibition of mitochondrial respiration depends on the length of preincubation with MPP^+ or its analogs (16, 17). For the convenience of comparison with previous work, the values given in Table 1 refer to 5 minute preincubation, at which time the concentration inside the mitochondria of most (but not necessarily all) MPP^+ analogs is approaching its maximum (16). It should be noted that maximum accumulation by the mitochondria does not mean that inhibition has reached a maximum. Penetration to one of the inhibitory sites can take much longer (17). The effect of TPB^- on the inhibition observed after 5 minutes of incubation is also shown in Figure 2 (open symbols). TPB^- is known to potentiate the inhibitory effect of MPP^+ and most of its analogs (18, 19) by accelerating their electrochemical equilibration across the mitochondrial membrane and by facilitating their penetration into the hydrophobic inhibition site on NADH dehydrogenase (17). As for MPP^+, TPB^- both accelerates the onset of inhibition and changes the observed partial inhibition to complete inhibition.

Table 1 summarizes the inhibitory effect of the MSP^+ analogs on state 3 respiration in mitochondria oxidizing NAD^+-linked substrates. Table 1 also shows that the inclusion of 10 μM TPB^- lowers the IC_{50} value. Although the effect is not nearly as dramatic as with MPP^+, the IC_{50} is lowered by one and a half orders of magnitude, with the exception of 1-methyl-4-(α-naphthylethenyl)-pyridinium. The lesser potentiation by TPB^- of the inhibition by the MSP^+ analogs in general and the naphthyl compound in particular is most likely due to their being more hydrophobic than MPP^+. We have reported (4) that for a series of 4′-alkyl-MPP analogs, the more hydrophobic the compound, the less effective TPB^- was in lowering the IC_{50} value for the inhibition of NADH oxidation in inner membranes.

Inhibition of NADH Oxidation in Inner Membrane Preparations

The inhibition of NADH oxidase in ETP by MPP^+ and its analogs is the result of their binding to two inhibitory sites (17). One of these equilibrates readily with the aqueous medium, but occupancy of this site results in only partial (35–40%) inhibition. When both sites are filled, complete inhibition is observed. The second site is thought to be located in a hydrophobic environment, which hydrophobic MPP^+ analogs, such as 4′-decyl MPP^+ or 4-phenylpyridine penetrate readily. At or near this hydrophobic binding site, two ionizable groups influence inhibition by charged analogs only. Binding is favored when these groups are deprotonated (17).

TPB^- forms strong ion pairs with positively charged MPP^+ analogs. The resulting ion pairs enter the hydrophobic binding site rapidly, partly because of the increased hydrophobicity, and partly because they are electrically neutral. This is thought to be the mechanism whereby a catalytic amount of TPB^- greatly ac-

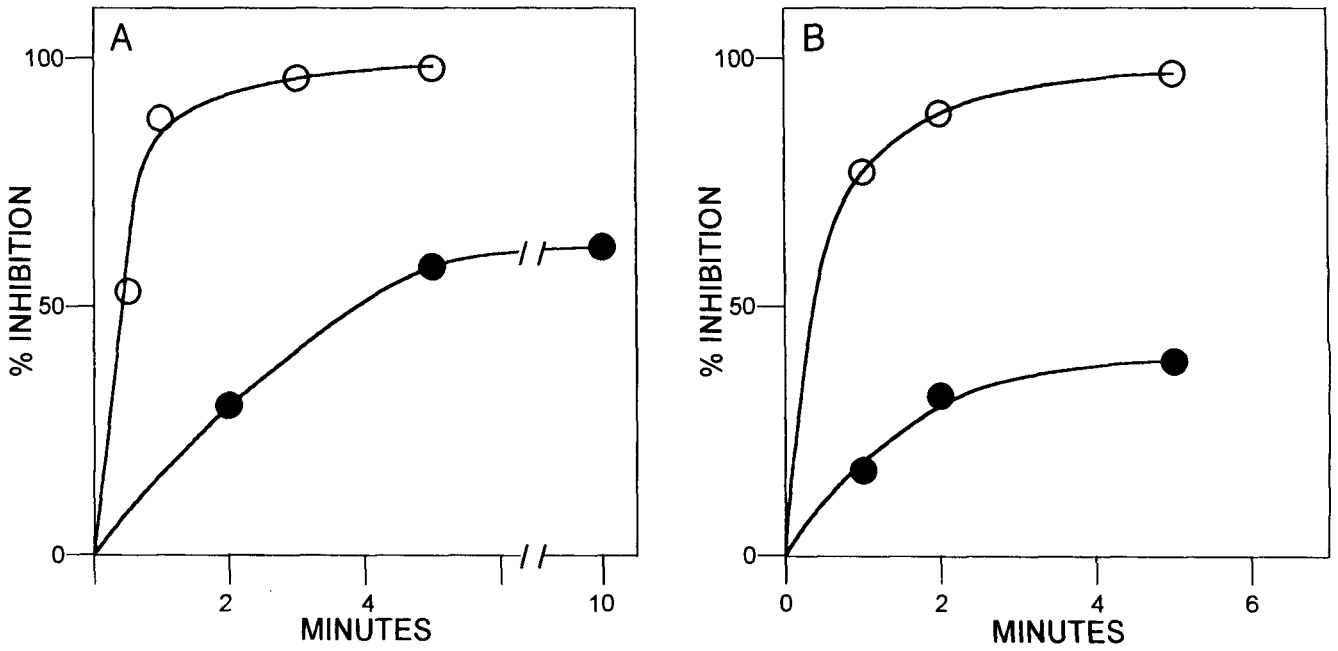

FIGURE 2. Time dependence of the inhibition of malate and glutamate oxidation in mitochondria in state 3 by 1,1-dimethyl-1,2,3,6-tetrahydrostilbazole. The time scale on the abscissa denotes the time of preincubation of the mitochondria with the inhibitor at 30° prior to the addition of substrate and ADP. The concentration of the inhibitor was 360 μM in A and 180 μM in B. Solid circles, no TPB^-; open circles, with 10 μM TPB^- present. The inhibitor was dissolved in 50% (v/v) ethanol and diluted to 0.5% final alcohol concentration in experiment A and to 0.25% in B.

TABLE 1. Inhibition of Mitochondrial Respiration and NADH Oxidation in Submitochondrial Particles by 1-Methylstyrylpyridiniums and Related Compounds

	IC_{50} (μM)			
	Mitochondria		*ETP*	
Compound	*−TPB*	*+TPB*	*−TPB*	*+TPB*
MPP^+	193	2.6	3300	825
MSP^+	53	3.6	140	75
2′-Me-MSP^+	14	0.30	125	50
2′-MeO-MSP^+	15	0.25	175	150
4′-CH_3-MSP^+	8.9	0.15	210	19
4′-MeO-MSP^+	15	0.25	220	66
4′-F-MSP^+	39	0.42	>300	110
4′-Br-MSP^+	42	10	950	42
4′-dimethylamino-MSP^+	2.5	0.08	250	60
2′,3′-diMeO-MSP^+	75	4.0	1500	175
1-Et-SP^+	50	2.5	700	100
1-Bz-SP^+	25	0.6	54	15
1-Me-4-(α-naphthylethenyl)-P^+	5.2	4.5	90	15
1-Me-4-(α-ferrocenylethenyl)-P^+	45	4.0	600	100
1-Me-4-(phenylethyl)-P^+			*a*	400
1,1-diMe-THS	290	24	1000	30

The structures of the parent compounds are given in Figure 1.
[a]Inhibition weak and partial at solubility limit. IC_{50} values for MPP^+ inhibition in intact mitochondria are from Reference 18.

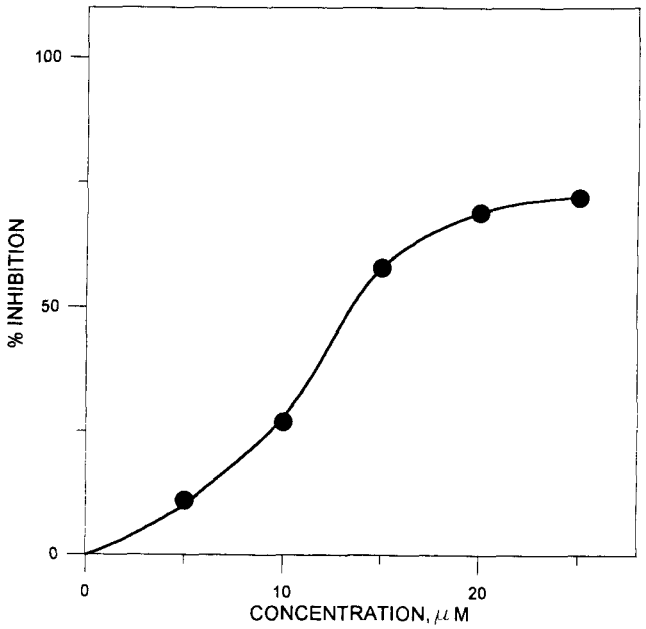

FIGURE 3. Sigmoidal behavior of inhibition of NADH oxidase activity by 1-benzyl-4-styrylpyridinium in an ETP preparation in the presence of TPB^-. The abscissa denotes the concentration of the inhibitor. TPB^- (10 μM) was present in all samples. Preincubation time, 5 minutes at 30°.

celerates the attainment of inhibition by charged, relatively hydrophilic compounds, as well as lowers the IC_{50} value in inner membrane preparations. If the concentration of TPB^- equals or exceeds that of the added inhibitor, however, it hinders the inhibition by competing with the hydrophobic binding site for the inhibitor and may even reverse the inhibition (17). The sigmoidal titration curves observed with some inhibitors in the presence of TPB^- may be due to such competition. Figure 3 illustrates the sigmoidal titration curves obtained under conditions where the concentration of added TPB^- (10 μM) equals or exceeds that of the inhibitor. The incomplete inhibition observed with the compound used here (*N*-benzyl-4-styrylpyridinium) may reflect the difficulty that the bulky ion pair formed between TPB^- and this compound has in entering the external, hydrophilic site, leaving only the hydrophobic one completely occupied.

The IC_{50} values for the inhibition of NADH oxidation by MSP^+ derivatives summarized in Table 1 are in accord with the general model proposed in Reference 17 and outlined above. Keeping in mind that the IC_{50} values given in the table are not absolute but reflect the inhibition attained after 5 minutes of preincubation of the submitochondrial particles with the particular inhibitor (though only in a few cases was a small increase in inhibition found after 5 minutes of incubation without TPB^-), it is apparent that the IC_{50} values are one or two orders of magnitude higher in ETP than in mitochondria. This is as expected, since the MSP^+ analogs, like MPP^+ analogs, are concentrated in the mitochondrial matrix by the electrochemical gradient, so that the actual concentration in the matrix far exceeds the added concentration, whereas in ETP, being an inverted membrane, this does not occur. IC_{50} values in mitochondria thus include both kinetic and thermodynamic parameters, whereas in ETP they are purely kinetic. Thus, as discussed elsewhere (16), the values in mitochondria and ETP are not strictly comparable.

The IC_{50} values for the MSP^+ series in Table 1 are all an order of magnitude lower than for the corresponding MPP^+ analogs. Thus, the IC_{50} for MPP^+ has been reported as 3300 μM without and 825 μM with 10 μM TPB^-; for 2′-Me-MPP^+ 4100 without TPB; for 4′-Me-MPP^+ 680 μM without and 190 μM with TPB^- present; and for 2′-MeO-MPP^+ and 4′-Fl-MPP^+ in the absence of TPB^- 1200 and 2000 μM, respectively (16, 17). It would seem from comparison of these figures with the values in Table 1 that the additional hydrophobicity, imparted by the insertion of an ethylene bridge, favors binding to NADH dehydrogenase. The same trend is suggested by the dramatic increase in the IC_{50} value when the benzene ring of MSP^+ is replaced with the polar methylpyridinium moiety (Table 1).

Inhibition of NADH oxidation in ETP by MSP^+ and its analogs showed only a modest or no time dependence. Where a slight increase in inhibition was noted when incubation with the inhibitor was continued for 60 minutes, it was abolished by TPB^-, lowering the IC_{50} value to a lesser extent than with most MPP^+ analogs (Table 1). This behavior may be ascribed to the fact that the positive charge on the nitrogen is greatly delocalized in MSP^+, and thus the inhibitor can enter the membrane relatively easily.

The data presented here are fully compatible with the concept of dual binding sites for inhibitors which block electron transport between NADH dehydrogenase and Q. Together with recently published data describing the characteristics of inhibition by 4′-alkyl derivatives of 4′-phenylpyridine and MPP^+ (17), they provide a starting point for attempting to describe the molecular parameters which determine the effectiveness of inhibitors acting at the "rotenone sites."

Quantitative Structure Activity Relations

Several studies of compounds structurally related to MPP^+ have been carried out in an effort to identify environmental and endogenous compounds which might inhibit NADH dehydrogenase in vivo and also lead to endogenous Parkinson's disease. These structure-function studies (16, 17, 20) have identified some common properties which make the compounds good inhibitors of NADH dehydrogenase. These properties include hydrophobicity and the presence of a positively charged nitrogen in the case of pyridine derivatives. However, such comparative studies cannot be extrapolated to predict the efficacy of remotely related and unrelated compounds. We sought to use the accumulated information from the structure-function studies to predict efficacy based solely on selected molecular descriptors for compounds outside the series of homologs that have been studied. Such a tool would be useful for predicting whether novel drugs or their metabolic products or endogenous metabolic intermediates might be deleterious to the energy metabolism in the cell.

To this end, we used the EMMA program, a QSAR software developed in and commercially available from the Chemistry Department of Moscow State University* to quantitate the relationship between molecular properties and experimentally determined biological activity. Molecular properties are represented via combinations of standard topological, physicochemical, and structural descriptors selected by the program on the basis of the structural formula of the compound.

*A detailed explanation of the program and licensing are available from the same source.

The program was applied in two stages. In the first stage, we selected 25 MSP^+, MPP^+, and 4-phenylpyridine derivatives for which reliable equilibrium IC_{50} values were available for the inhibition of the enzyme in ETP preparations. The values were taken from a recent article by Gluck et al. (17) and from Table 1, since most earlier data reported in the literature represent values after 5 minutes of incubation and thus were not determined at equilibrium. Of the 25 compounds selected, the structural formulas of 22 were entered into the program, along with their IC_{50} values in the absence and the presence of 10 μM TPB^-. The program then generated numerous models in the form of regression equations. The remaining three compounds were used as if their IC_{50} values had not been known, i.e., the program predicted their IC_{50} values, which were then compared with the published values. In this manner, two models were chosen (one, denoted as A_1, representing the IC_{50} value in the absence of TPB^-, the other, denoted as A_2, representing the IC_{50} in the presence of 10 μM TPB^-) which predicted most closely the known IC_{50} values of the three test compounds on the basis of a correlation coefficient >0.9 and satisfactory values for Fisher's criteria. The regression equations thus selected were as follows:

$$A_1 = 1.59 - 0.53\,N - 0.13\,ArB + 0.14\,CC + 1.24\,CCCar$$

where N, ArB, CC, and CCCar are formal structural descriptors characterizing the presence of the quaternary N atom and the presence of fragments carrying lipophilic properties, such as aromatic bond, carbon–carbon fragment, and CH_2–CH_2–C (aromatic), respectively.

$$A_2 = 45.14 - 1.98BJ + 0.22LS + 8.42Pm + 361.5Bm$$

where BJ is Balaban's J index (22); LS is the lowest electropological state index (23) of atoms N in molecule; and Pm and Bm are minimal diagonal elements from B matrix and minimal nondiagonal element of B matrix, respectively, as defined in Reference 24. All these are topological parameters which reflect shape and size of the molecule.

In the second stage these two models were used to predict the IC_{50} values of 12 novel compounds that had not been studied previously for inhibitory capacity. In this manner we hoped to obtain an indication of the general applicability of these models for predicting the effectiveness of reversible inhibitors which might act at the rotenone sites.

The structures of the 12 test compounds are shown in Figure 4. Note that they represent a wide range of structural variation and that some (e.g., numbers **9** and **10**) resemble MPP^+ fairly closely, while others lack the benzene ring or both the benzene and pyridinium rings (number **3**).

Prior to presenting the results of the application of the EMMA program to the novel compounds represented in Figure 4, the characteristics of the inhibition elicited by these compounds need to be discussed. Figure 5 illustrates the variations in the behavior of the test compounds as inhibitors of NADH oxidation and highlights several of the problems encountered in the QSAR analysis to be presented in Table 2. Figure 5A demonstrates that compound **11**, a relatively hydrophobic inhibitor, rapidly enters both inhibition sites, because maximal inhibition is reached in 5 minutes and, accordingly, TPB^- has no effect. Figure 5B illustrates the behavior of a compound which, like MPP^+, causes partial (~40%) inhibition in 5 minutes and even after 2 hours of incubation yields incomplete inhibition, but a catalytic amount of TPB^- greatly accelerates the process and lowers the apparent IC_{50}. The compound used in Figure 5C is between these extremes: Although in the absence of TPB^-, equilibrium is not reached in 5 minutes, the titration curves at 2 hours in the absence of TPB^- and at 5 minutes in the presence of 10 μM TPB^- are superimposable; consequently, the IC_{50} values are identical, and equilibrium has been reached. Figure 5D shows a behavior similar to that seen in 5C, except in one important respect: 10 μM TPB^- does not accelerate the development of the inhibition by compound **1**, perhaps because the quaternary nitrogen is too crowded for tight ion pairing with TPB^-. Thus, the inhibition with TPB^- present at 5 minutes is clearly not an equilibrium value. The sigmoidal titration curve seen in the presence of TPB^- cannot be ascribed to strong binding of the inhibitor by TPB^- in this instance, especially since the concentration of the latter far exceeded that of the TPB^-.

The observed IC_{50} values determined in the absence and the presence of TPB^- are reported in Table 2. Without TPB^- all but two compounds, numbers **5** and **9**, had reached equilibrium. Despite the agreement between observed and predicted IC_{50}s for compound **5**, its interaction with the inhibition site was not complete in 2 hours, as seen in Figure 5B and confirmed by the fact that the IC_{50} value with 10 μM TPB^- present was considerably lower. For similar reasons, the apparent IC_{50} for compound **9** is also not an equilibrium value.

In the second stage of testing the program, the structures of the 12 compounds in Figure 4 were entered into the EMMA program, which then generated values for the two mathematical models selected so as to predict the IC_{50} values for each in the absence and presence of TPB^-. The correlation between the observed and predicted values was quite satisfactory (Table 2), despite the divergences in the structures of the MPP^+, MSP^+, and 4-phenylpyridine analogs used to develop the models and those of the test compounds

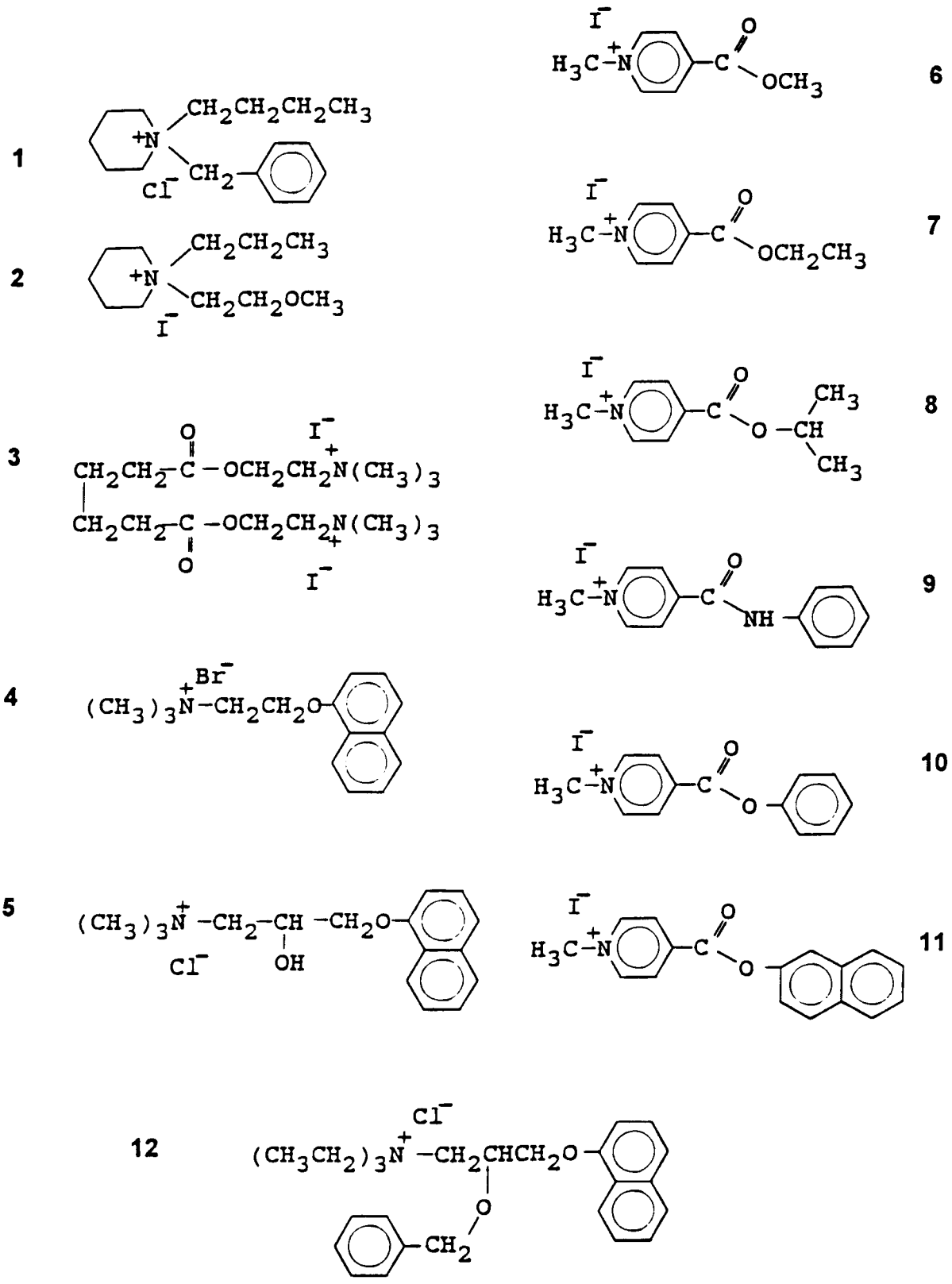

FIGURE 4. Structures of the novel inhibitors used in the experiments of Table 3.

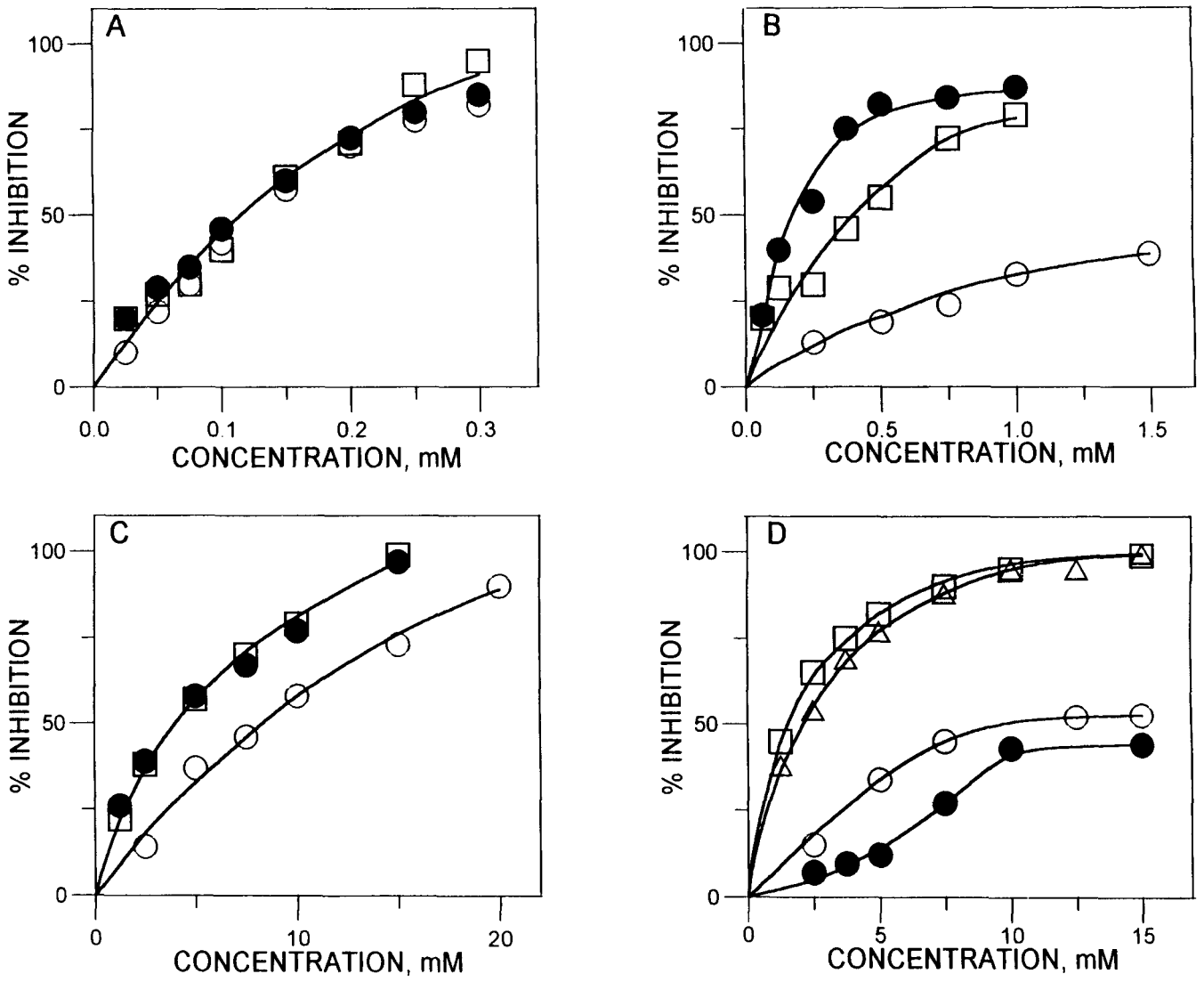

FIGURE 5. *Variations in the development of the inhibition of NADH oxidase activity by the compounds shown in Figure 4. Symbols: open circles, 5 minutes preincubation of the inhibitor with ETP at 30° without TPB⁻; closed circles, 5 minutes with 10 μM TPB⁻ present; triangles, 60 minute preincubation with or without 10 μM TPB⁻; open squares, 120 minute preincubation without TPB⁻. The enzyme used was an ETP preparation, and assays were spectrophotometric, except in A, where the polarographic assay was used because of interference by turbidity. The inhibitors used were A, compound* **11** *of Figure 4, dissolved in 50% (v/v) dimethylsulfoxide (final concentration in assay = 1%); B, compound* **5**; *C, compound* **6**; *and D, compound* **1**.

(Figure 4). Figure 6 shows the correlation for the IC_{50} values in the absence of TPB^-. Using only the nine compounds which reached equilibrium, the correlation coefficient was 0.943. Figure 7 shows the analogous correlation for the IC_{50} in the presence of TPB^-. The r value for the six compounds which were clearly at equilibrium was found to be 0.928. The satisfactory correlation between the predicted and experimental values, despite the major structural differences between the test compounds and the MPP^+ and MSP^+ analogs on which the models were based, suggests that such models may be useful in predicting the reactivity of other inhibitors with the rotenone sites in Complex I.

DISCUSSION

The nonflexible MPP^+ analogs, MSP^+ and its derivatives, which were the subject of the present investigation, inhibit mitochondrial respiration on NAD^+-linked substrates and NADH oxidation in an inverted inner membrane preparation (ETP). In both systems, they are considerably more inhibitory than the corre-

TABLE 2. Predicted and Observed IC_{50} Values for a Series of Novel Inhibitors of NADH Dehydrogenase

	IC_{50} (mM)					
	Without TPB			With 10 μM TPB		
Compound[a]	Predicted	Observed	Equilibrium reached	Predicted	Observed	Equilibrium reached
1	0.40	1.5	Yes	0.07	10	No
2	2.5	1.5	Yes	0.36	4.5	No
3	2.5	4.5	Yes	0.41	10	No
4	0.60	0.23	Yes	0.58	0.59	No
5	0.44	0.43	Nearly	0.42	0.20	Yes
6	2.8	4.0	Yes	2.6	4.0	Yes
7	2.1	4.0	No	1.5	2.5	Yes
8	1.5	1.0	Yes	1.4	1.0	Yes
9	0.50	2.3	No	0.50	0.55	Yes
10	0.45	0.27	Yes	0.80	1.26	?
11	0.10	0.12	Yes	0.08	0.12	Yes
12	0.02	0.025	Yes	0.19	0.17	?

[a]For structures of these compounds, see Figure 4.

IC_{50} values for NADH oxidation in ETP were determined at 30° spectrophotometrically, except for compounds **4, 5,** and **11,** which were assayed polarographically because of interference by the absorbance of the inhibitor at 340 nm. Replicate assays agreed ±5%.

Values without TPB^- present refer to 2 hours of preincubation of the submitochondrial particles with the inhibitor at 30°, those with TPB^- refer to 5 minutes of preincubation with the inhibitor.

In samples without TPB^-, "No" in the equilibrium column denotes the fact that at 2 hours complete inhibition was not reached at any inhibitor concentration.

In samples with TPB^- present, "No" denotes the fact that the apparent IC_{50} decreased further on continued incubation beyond 5 minutes and "?" denotes uncertainty about equilibrium because the IC_{50} with and without TPB^- were significantly different.

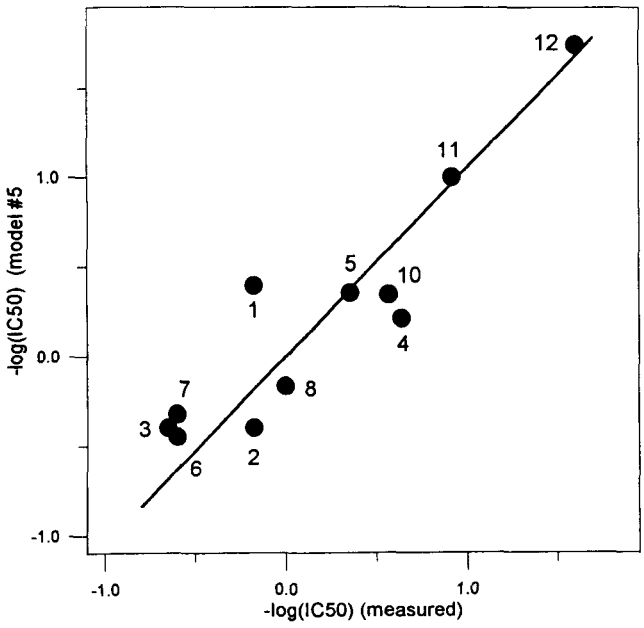

FIGURE 6. Correlation of predicted and observed values of IC_{50} (μM) in the absence of TPB^-. The numbers identify the compound in Figure 4. The procedure used to arrive at the predicted values is given in the text, and the values are taken from Table 2. For the nine compounds where equilibrium was reached, $r = 0.943$.

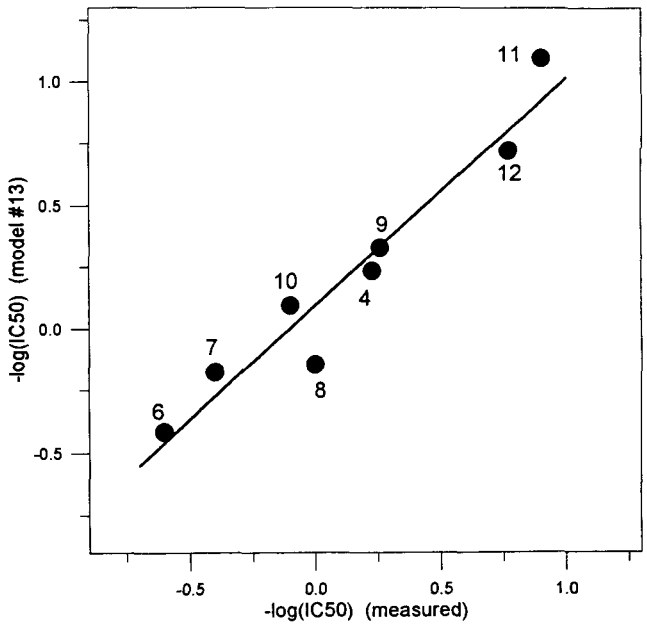

FIGURE 7. Correlation of predicted and observed values of IC_{50} (μM) in the presence of TPB^-. The numbers identify the compound in Figure 4. The correlation coefficient $r = 0.928$.

sponding MPP^+ analogs, in line with expectation from their more hydrophobic nature. In ETP, the IC_{50} values reflect only one process, namely, the equilibrium with the inhibitory sites in Complex I. For this process, substitution to the phenyl ring did not much change the IC_{50} values, although bulky substituents (e.g., 4'-Br or 2'-3'-dimethoxy) resulted in slightly higher concentra-

tions required for 50% inhibition in the absence of TPB^-. In contrast, for mitochondria, 4'-substitution greatly decreased the IC_{50}, particularly in the presence of TPB^- (by 10-fold). Lipophilic groups (methyl and methoxy) decreased the IC_{50} both in the presence and in the absence of TPB^-. In mitochondria two processes contribute to the measured IC_{50}, namely, the accumulation into the matrix in response to the electrical gradient across the inner membrane and the equilibration with the inhibitory sites. Thus, differences between the two preparations can at least in part be ascribed to the accumulation step which alters the effective local concentration. The best inhibitor of mitochondrial respiration in this class was the dimethylamino derivative with IC_{50} values of 2.5 μM without TPB^- (20-fold lower than MSP^+ itself) and 0.08 μM in the presence of TPB^- (45-fold lower than MSP^+).

Some of the MSP^+ derivatives and the parent MTHS compounds have been examined for dopaminergic neurotoxicity in a cell culture system of mesencephalic neurons (personal communication from Dr. William J. Nicklas). In contrast to flexible MPP^+ analogs with one to three methylene groups between the aromatic and pyridine rings, none of which were found to be neurotoxic in that study, several MTHS and MSP^+ derivatives showed measurable neurotoxicity but were considerably less effective than the corresponding MPP^+ derivatives. The lesser neurotoxicity of MSP^+ and its derivatives may be, at least in part, due to poor uptake by the dopamine carrier, as suggested by a published report (21) that MSP^+ derivatives are ineffective as competitive inhibitors of (^{14}C)-dopamine uptake by synaptosomes from mouse brain.

Using the equilibrium IC_{50} data for the inhibition of NADH oxidation in ETP by MSP^+ derivatives (Table 1) and previously reported data for MPP^+ and 4-phenyldpyridine derivatives, a QSAR analysis was undertaken with the goal in mind of developing a mathematical model for predicting the inhibitory potency of as yet untested potential inhibitors acting at the rotenone sites. To this end, models were developed with the help of a proprietary QSAR program, the EMMA software. Two mathematical models were selected, as best fitting the experimentally observed IC_{50} values of 3 MPP^+ and MSP^+ analogs, one in the presence and the other in the absence of TPB^-. These mathematical models were then applied to predicting the IC_{50} values of 12 novel compounds with structural divergences from MPP^+ and MSP^+ varying from significant to very extensive. The satisfactory correlation obtained for these test compounds between predicted and observed values offers hope that this approach may be useful in predicting the inhibitory potency of drugs, metabolites, and toxins expected to interact with the rotenone sites.

ACKNOWLEDGMENTS

This investigation was supported by the National Institutes of Health (HL-16251) and the Department of Veteran Affairs.

REFERENCES

1. S. K. Youngster, K. A. McKeown, Y.-Z. Jin, R. R. Ramsay, R. E. Heikkila, and T. P. Singer (1989). Oxidation of analogs of 1-methyl-4-phenyl-1,2,3,6-tetrahydropyridine by monoamine oxidases A and B and the inhibition of monamine oxidases by the oxidation products. *J. Neurochem.*, **53,** 1837–1842.
2. R. R. Ramsay, J. I. Salach, and T. P. Singer (1986). Uptake of the neurotoxin 1-methyl-4-phenylpyridine (MPP^+) by mitochondria and its relation to the inhibition of mitochondrial oxidation of NAD^+-linked substrates by MPP^+. *Biochem. Biophys. Res. Commun.*, **134,** 743–748.
3. R. R. Ramsay, M. J. Krueger, S. K. Youngster, and T. P. Singer (1991). Evidence that the inhibition sites of the neurotoxic amine 1-methyl-4-phenylpyridinium (MPP^+) and the respiratory chain inhibitor, piericidin A, are the same. *Biochem. J.*, **273,** 481–484.
4. R. R. Ramsay, M. J. Krueger, S. K. Youngster, M. R. Gluck, J. E. Casida, and T. P. Singer (1991). Interaction of 1-methyl-4-phenylpyridinium ion (MPP^+) and its analogs with the rotenone/piericidin binding site of NADH dehydrogenase. *J. Neurochem.*, **56,** 1184–1190.
5. W. J. Nicklas, I. Vyas, and R. E. Heikkila (1985). Inhibition of NADH-linked oxidation in brain mitochondria by 1-methyl-4-phenylpyridine, a metabolite of the neurotoxin, 1-methyl-4-phenyl-1,2,5,6-tetrahydropyridine. *Life Sci.*, **36,** 2503–2508.
6. R. R. Ramsay, A. T. Kowai, M. K. Johnson, J. I. Salach, and T. P. Singer (1987). The inhibition site of MPP^+, the neurotoxic bioactivation product of 1-methyl-4-phenyl-1,2,3,6-tetrahydropyridine is near the Q-binding site of NADH dehydrogenase. *Arch. Biochem. Biophys.*, **259,** 645–649.
7. T. P. Singer, N. Castagnoli, R. R. Ramsay, and A. J. Trevor (1987). Biochemical events in the development of Parkinson's disease induced by 1-methyl-4-phenyl-1,2,3,6-tetrahydropyridine. *J. Neurochem.*, **49,** 1–8.
8. L. M. Sayre (1989). Biochemical mechanism of action of the dopaminergic neurotoxin 1-methyl-4-phenyl-1,2,3,6-tetrahydropyridine (MPTP). *Toxicol. Lett.*, **48,** 128–149.
9. S. K. Youngster, P. K. Sonsalla, and R. E. Heikkila (1987). Evaluation of the biological activity of several analogs of the dopaminergic neurotoxin 1-methyl-4-phenyl-1,2,3,6-tetrahydropyridine. *J. Neurochem.*, **48,** 929–934.
10. S. O. Sablin, M. J. Krueger, T. P. Singer, S. O. Bachurin, A. B. Khare, S. M. N. Efange, and S. E. Tkachenko (1994). Interaction of tetrahydrostilbazoles with monoamine oxidase A and B. *J. Med. Chem.*, **37,** 151–157.
11. M. J. Krueger, S. M. N. Efange, R. H. Michelson, and T. P. Singer (1992). Interaction of flexible analogs of N-methyl-4-phenyl-1,2,3,6-tetrahydropyridine and of N-methyl-phenylpyridinium with highly purified monoamine oxidase A and B. *Biochemistry*, **31,** 5611–5615.
12. S. M. N. Efange, R. H. Michelson, A. K. Tan, M. J. Krueger, and T. P. Singer (1993). Molecular size and flexibility as determinants of selectivity in the oxidation of N-

methyl-4-phenyl-1,2,3,6-tetrahydropyridine analogs by monoamine oxidase A and B. *J. Med. Chem.*, **36,** 1278–1283.
13. C. Schnaitman and J. W. Greenawalt (1968). Enzymatic properties of the inner and outer membranes of liver mitochondria. *J. Cell Biol.*, **38,** 158–175.
14. F. L. Crane, J. L. Glenn, and D. E. Green (1956). Studies on the electron transport system IV. The electron transport particle. *Biochim. Biophys. Acta*, **22,** 475–487.
15. T. P. Singer (1974). Determination of the activity of succinate, NADH, choline, and α-glycerophosphate dehydrogenases. *Meth. Biochem. Anal.*, **22,** 123–175.
16. R. R. Ramsay, S. K. Youngster, W. J. Nicklas, K. A. McKeown, Y.-Z. Jin, R. E. Heikkila, and T. P. Singer (1989). Structural dependence of the inhibition of mitochondrial respiration and of NADH oxidase by N-methyl-4-phenylpyridinium (MPP^+) and the energized accumulation in mitochondria. *Proc. Natl. Acad. Sci. U.S.A.*, **86,** 9168–9172.
17. M. R. Gluck, M. J. Krueger, R. R. Ramsay, S. O. Sablin, T. P. Singer, and W. J. Nicklas (1994). Characterization of the inhibitory mechanism of 1-methyl-4-phenylpyridinium and 4-phenylpyridine analogs in inner membrane preparations. *J. Biol. Chem.*, **269,** 3167–3174.
18. R. R. Ramsay, R. J. Mehlhom, and T. P. Singer (1989). Enhancement by tetraphenylboron of the interaction of the 1-methyl-4-phenylpyridinium ion (MPP^+) with mitochondria. *Biochem. Biophys. Res. Commun.*, **159,** 983–990.
19. R. E. Heikkila, J. Hwang, S. Ofori, H. M. Geller, and W. J. Nicklas (1990). Potentiation by the tetraphenylboron anion of the effects of 1-methyl-4-phenyl-1,2,3,6-tetrahydropyridine and its pyridinium metabolite. *J. Neurochem.*, **54,** 743–750.
20. C. L. Hoppel, D. Greenblatt, H.-C. Kwok, P. K. Arora, M. P. Singh, and L. M. Sayre (1987). Inhibition of mitochondrial respiration by analogs of 4-phenylpyridinium and 1-methyl-4-phenylpyridinium cation (MPP^+), the neurotoxic metabolite of MPTP. *Biochem. Biophys. Res. Commun.*, **148,** 684–692.
21. S. O. Bachurin, N. N. Lemontova, S. O. Sablin, L. S. Solyakov, and S. E. Tkachenko (1992). Biochemical basis of structural electivity of MPTP-like neurotoxicity. Neurotoxin and their potential role in neurodegeneration. *Ann. N. Y. Acad. Aci.*, **648,** 248–250.
22. A. T. Balaban (1983). Topological indices based on topological distances in molecular graphs. *Pure Appl. Chem.*, **55,** 199–206.
23. L. B. Kier and L. H. Hall (1990). An electropological-state index for atoms in molecules. *Pharmaceutical Res.*, **7,** 801–807.
24. S. S. Tratch, R. O. Devdariani, and N. S. Zefirov (1990). Combinatoric models and algorithms in chemistry. Topologico- conficurational analogs of the Weiner's index. *Zhumal Organicheskoi Khimii (Russ.)*, **26,** 921–932.